Low-Temperature Drop-on-Demand Reactive Silver Inks for Solar Cell Front-Grid Metallization

April M. Jeffries, Avinash Mamidanna, Laura Ding, Owen J. Hildreth, and Mariana I. Bertoni

***Abstract*—Formation of high-conductivity metal contacts at low temperatures expands optoelectronic device opportunities to include thermally sensitive layers, while reducing expended thermal budget for fabrication. This includes high-efficiency silicon heterojunction solar cells with intrinsic amorphous silicon layers. Efficiencies of these cells are limited by series resistance; the primary cause of this is the relatively high resistivity of the low-temperature silver paste used to form front-grid metallization. In this paper, we report the formation of highly conductive features by drop-on-demand printing of reactive silver ink (RSI) at a low temperature of 78 °C, resulting in media resistivities of 3–5 $\mu\Omega$·cm. When used as a front grid on a silicon heterojunction solar cell, RSI fingers give cell series resistance of 1.8 Ω·cm^2 (without optimization of the process), which is impressively close to 1.1 Ω·cm^2 for our commercially available screen-printed low-temperature silver paste metallization. We present here the promising first results of RSI as metallic finger for photovoltaics, which upon optimization of design parameters has the potential to outperform the screen-printed low-temperature silver paste counterpart.**

***Index Terms*—Contacts, drop-on-demand printing, low-temperature metallization, metallization, silver usage.**

I. Introduction

LOW-RESISTANCE ohmic contact formation often requires high temperatures in order to evaporate conductivity-limiting organic residues in conductive pastes or to sinter conductive particles [1], [2]. Unfortunately, these high temperatures are incompatible with many emerging technologies that include thermally sensitive substrates or layers, including flexible lightweight wearable electronics printed on polymer, cloth or paper substrates, or high-efficiency solar cells [1]–[4]. Formation of high-conductivity metallization readily at mild temperatures broadens device application opportunities to include thermally sensitive substrates and electronically active layers.

Manuscript received July 5, 2016; revised August 30, 2016; accepted October 3, 2016. Date of publication November 23, 2016; date of current version December 20, 2016. This work was supported in part by the Engineering Research Center Program of the National Science Foundation (NSF) and the Office of Energy Efficiency and Renewable Energy of the Department of Energy under NSF Cooperative under Agreement EEC-1041895, Science Foundation Arizona under Grant BSP 0615-15, and by the U.S. Department of Energy, Energy Efficiency, and Renewable Energy Program, under Award DE-EE0006335.

A. M. Jeffries, A. Mamidanna, and O. J. Hildreth are with the School for Engineering of Matter, Transport, and Energy, Arizona State University, Tempe, AZ 85281 USA (e-mail: april.jeffries@asu.edu; amamidan@asu.edu; owen.hildreth@asu.edu).

L. Ding and M. I. Bertoni are with the School of Electrical, Computer and Energy Engineering, Arizona State University, Tempe, AZ 85281 USA (e-mail: laura.ding@asu.edu; bertoni@asu.edu).

Color versions of one or more of the figures in this paper are available online at http://ieeexplore.ieee.org.

Digital Object Identifier 10.1109/JPHOTOV.2016.2621351

Reactive metallic inks—such as nickel, copper, and silver—enable drop-on-demand (DoD) printing of highly conductive features at low temperatures (typically 35–120 °C) without the need for a postdeposition anneal [1], [5], [6]. Reactive silver inks (RSI) are particularly attractive because Ag has the lowest electrical resistivity of all metals, and its oxides are also reasonably conductive; therefore, surface oxidation does not degrade performance as much as it does in a copper or nickel metallization [7]. In our work, RSI films were synthesized from silver acetate, formic acid, and ammonia following a modified Tollens' process, described in detail by Walker and Lewis [1]. The printing process from this ink results in the reduction and precipitation of Ag among residual acetate groups. Maintaining the substrate at mild temperatures below 100 °C during ink deposition favors volatilization of the organic residues, resulting in RSI films exhibiting composition and conductivity nearly equivalent to that of pure Ag [1], [6].

Metallization also often requires patterning of micrometer-size features for optimal device performance, which can advantageously be addressed by DoD RSI printing. This technique facilitates high-precision patterning of fine features without the need of additional masking steps, while also minimizing waste of precious metals in inks [8]. Here, we investigate RSI metallization deposited by DoD printing as front-grid metallization of solar cells, which, to our knowledge, is reported for the first time.

Currently, the solar market is dominated by Si technology, predominantly diffused-junction solar cells that over the last decade exhibited a drastic increase in efficiency while lowering cost per watt [9]. The highest efficiency for nonconcentrated Si solar cells is held by amorphous Si (a-Si)/crystalline Si (c-Si) heterojunction (SHJ) cells with a reported efficiency of 25.6% for standard reference spectra (ASTM G173) [3]. Screen-printing of low-cure-temperature Ag paste is the current standard metallization, as it is a low-cost high-throughput process. However, a performance limitation of SHJ cells is the considerably high series resistance (R_s) that primarily results from the relatively high-resistivity low-temperature Ag paste that is used for front-grid metallization. Although low resistivities of $\sim$5 $\mu\Omega$·cm have been recently reported for state-of-the-art curing processes using screen-printed Ag pastes, there is still room for improvement [10].

While diffused-junction Si solar cells can use high-temperature annealing to form low-resistance metallization from Ag pastes, SHJ cells are substantially more thermally sensitive, as the surface passivation—typically provided by hydrogenated amorphous silicon (a-Si:H)—begins to degrade at temperatures above $\sim$200 °C [11]. Therefore, a major hurdle

2156-3381 © 2016 IEEE. Personal use is permitted, but republication/redistribution requires IEEE permission.
See http://www.ieee.org/publications_standards/publications/rights/index.html for more information.

to achieving higher efficiency SHJ cells is in decreasing the overall R_s by reducing the metal resistivity and specific contact resistance. Our proposed combination of this advanced printing technique with RSI offers opportunities to benefit SHJ performance through

1) formation of highly conductive metallization grids to reduce series resistance;
2) processing at low temperatures to prevent degradation of thermally sensitive layers;
3) reduced front-grid feature size to minimize shadowing effects and enhance current generation.

Furthermore, these benefits are not only limited to SHJ solar cells, other thermally sensitive technologies such as organic photovoltaics, or flexible displays and antenna arrays could see improved performance using RSI metallization [12].

Additionally, DoD printing of RSI is economically compelling by potentially reducing the amount of Ag used and wasted in solar cell manufacturing [13], [14]. For DoD-printed RSI metallization, very little Ag is wasted. First, all of the printed Ag is directly used to form metallization with little waste occurring during nozzle cleaning, whereas some Ag paste is left on the screen following the conventional screen-printing process. Second, much finer features can be DoD printed; theoretically, screen-printed fingers on silicon solar cells typically 60–80 μm wide and 20–30 μm high could be replaced with smartwire on busbarless printed RSI fingers as thin as 35 μm and a few micrometers in height, which reduces silver consumption from about 100 to less than 10 mg per cell while maintaining high fill factors [9], [13], [15].

This work introduces and examines DoD printing of RSI ("DoD RSI") as an alternative front-grid metallization method for SHJ cells. First, we characterize the electrical and optical properties of DoD RSI films and compare them to those of commercially available screen-printed Ag paste ("SP paste") films. Second, modifications to DoD RSI metallizations such as features size and substrate morphology are discussed in relation to their influence on metal electrode properties. Then, the impact of front-grid metallization method on SHJ solar cell current–voltage characteristics is analyzed, with emphasis on the contributions to series resistance. Overall, similar performance is demonstrated for the SP paste and DoD RSI SHJ cell. Finally, a path toward DoD RSI optimization and exceeding the performance of SP paste is discussed.

II. Experiment

A. Reactive Silver Ink Synthesis

The base ink was prepared following Walker and Lewis' recipe [1]. All chemicals were used as received. 1.0 g of silver acetate ($C_2H_3AgO_2$, anhydrous 99%, Alfa Aesar) was dissolved in 2.5-mL ammonium hydroxide (NH_4OH, 28–30 wt%, ACS grade, BDH Chemicals). The solution was then stirred for 2 min on a vortex mixer to dissolve the silver acetate. Next, 0.2 mL of formic acid (CH_2O_2, ≥96%, ACS reagent grade, Sigma Aldrich) was added in two steps with a quick stir at the end of each step. The ink was then allowed to sit for 12 h before being filtered through a 450-nm nylon filter. For the experiments reported here, the RSI was diluted 1:1 by volume with ethanol (EtOH, C_2H_6O, ACS reagent grade, Sigma Aldrich) and then filtered again through the 450-nm nylon filter immediately before use.

B. Printing Process

RSI metallization features were printed in ambient atmosphere on a Microfab Jetlab II inkjet printing system described elsewhere [6]. The Jetlab II is equipped with an MJ-ATP-01 piezoelectric-driven print head with a 60-μm-wide nozzle. Samples were printed with the substrate held between 51 and 107 °C as measured using a k-type thermocouple in contact with the top surface of the substrate. The silver diamine ink was printed on the fly at 5 mm/s with 25-μm pitch (results in a 200-Hz ejection frequency). All DoD RSI metallizations were printed with five passes of the print head. SP paste grids were printed with an Applied Materials Baccini screen printer using a low-cure-temperature Ag paste from Namics Corporation.

C. Sample Preparation and Characterization

For media resistivity measurements by the four-point probe, 7×7 mm^2 pads were formed from SP paste and DoD RSI on electrically insulating substrates. For bulk optical property measurements by spectrophotometry, 2×2 cm^2 SP paste and DoD RSI pads were deposited on thin glass slides. The DoD RSI pads were printed at 51, 78, and 107 °C, whereas the SP paste contact pads were formed at room temperature and annealed in a muffle furnace in air for 20 min at 200 °C.

SHJ solar cell samples were fabricated from 5×5 in 180-μm-thick n-type CZ Si wafers. First, the wafers were chemically textured and cleaned using chemical baths of KOH, piranha, RCA-B, and buffered hydrofluoric acid solutions. Next, intrinsic and doped a-Si:H layers were deposited using plasma-enhanced chemical vapor deposition (Applied Materials P-5000). Cells were then defined by DC sputtering (Materials Research Corporation 944 sputtering system) deposition of tin-doped indium oxide (ITO) layers ($\sim$80 Ω/□) through a 2×2 cm^2 shadow mask. The back contact ITO and Ag were also DC sputtered as a full blanket. The complete stack and thicknesses are: ITO 70 nm/(p) a-Si:H 10 nm/(i) a-Si:H 6 nm/(n) c-Si 180 μm/(i) a-Si:H 6 nm/(n) a-Si:H 6nm/ITO 70 nm Ag 200 nm. Front grids were prepared on half of the samples by screen-printing a low-cure-temperature Ag paste (SP paste).

Next, all samples were annealed in air at 200 °C for 20 min in order to recover damage incurred during ITO sputtering deposition [16], in addition to curing the SP paste. Finally, front metallization was prepared according to the above-described RSI printing recipe at 78 °C on annealed SHJ cells.

Reflectance was measured from 300 to 1200 nm on a UV–vis–NIR spectrophotometer with an integrating sphere. Solar cell performances were characterized by one-sun and suns–V_{OC} current–voltage (*I–V*) measurements using a Sinton FCT-400 Series Light IV Tester. Surface morphology and cross-sectional thickness of the printed structures were characterized using field emission scanning electron microscope (SEM) at an accelerating voltage of 10.0 kV. The metal/ITO/Si specific contact

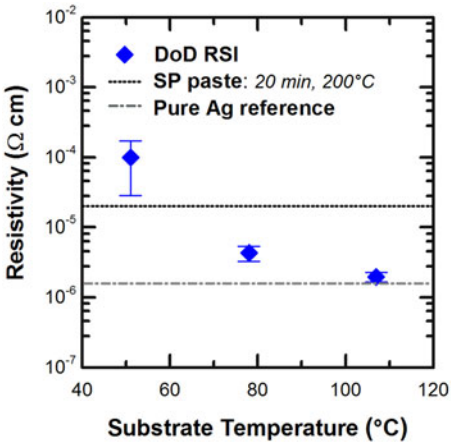

Fig. 1. Media resistivity of RSI-printed pads formed for various substrate temperatures compared with the resistivity of pure Ag, and SP Ag paste pads after curing for 20 min at 200 °C, showing that the media resistivity of RSI is lower than SP paste when printed at low temperatures.

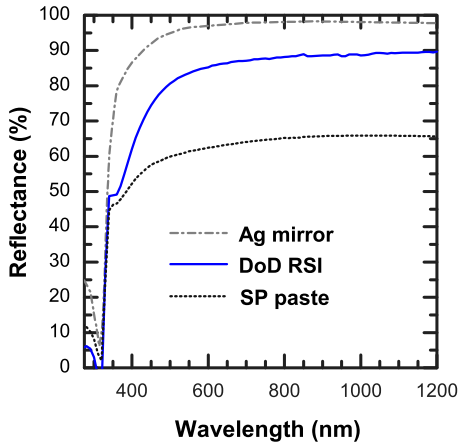

Fig. 2. Reflectance spectra of a DoD RSI metallization pad, an SP paste metallization pad, and a pure Ag mirror from [19].

resistance was assessed by the transfer length measurement (TLM) method.

III. Results and Discussion

First, we evaluate electrical and optical properties of large DoD RSI pads. Fig. 1 shows media resistivity of 7 × 7 mm^2 pads printed at various substrate temperatures, bulk resistivity of pure Ag (1.6 $\mu\Omega$·cm), and media resistivity of 7 × 7 mm^2 SP paste pads after curing for 20 min at 200 °C (20 $\mu\Omega$·cm). Here, the distinction is made between bulk resistivity and media resistivity, which is used to describe resistivity of a composite or a porous material [17]. As will be discussed later, the porosity of the RSI printed features forces electrical conduction to proceed through a network of interconnected particles, and hence, our reported media resistivity values reflect percolation-transport limitations to the actual resistivity [6], [17], [18]. At 51 °C, the DoD RSI pad exhibits an average media resistivity of 100 $\mu\Omega$·cm, five times higher than values of the SP paste pad. Some of our prior work was dedicated to fully assess the impact of various humectants, dilutions, and substrate temperatures on the electrical properties of DoD RSI-printed films [6]. These results, along with the work of others [1], [6], showed that DoD RSI films can reach extremely low media resistivities, close to that of bulk Ag. The RSI recipe we used here has ethanol as solvent, which has a boiling point of 78 °C. Upon increasing the substrate temperature to 78 °C, the DoD RSI pad media resistivity decreases with an average of 4.4 $\mu\Omega$·cm. This is only about 2.5 times the resistivity of pure bulk Ag and still an order of magnitude less resistive than metallization pads from cured SP paste. However, note that optimization of curing time and temperature of our SP paste might result in improved media resistivities. The media resistivity of RSI can approach that of pure Ag with removal of residual organics, which is accelerated as substrate temperature is elevated, optimally above 90 °C [1]. Heated at 78 °C, the RSI-printed pad likely still contains traces of these residuals, limiting bulk resistivity. We observe an even lower media resistivity of 2.0 $\mu\Omega$·cm for the RSI pad at a substrate temperature of 107 °C. Since the DoD RSI contact pads were deposited in ambient atmosphere, oxidation of Ag is expected to occur at elevated temperatures, resulting in media resistivity slightly higher than pure Ag. Furthermore, the DoD RSI pad has a porous structure. Moreover, the high surface area exposed to air in these porous RSI pads can favor oxidation and increased media resistivity. Therefore, resistivity of the DoD RSI metallization pads is expected to approach that of pure Ag by optimization of the substrate heating temperature to remove all residual organics, the RSI recipe to reduce porosity, and by printing in an inert atmosphere to eliminate oxidation at elevated temperatures.

Fig. 2 shows total reflectance spectra of 2 × 2 cm^2 pads formed from SP paste and DoD RSI compared with a smooth pure Ag mirror [19]. Transmittance measurements (not shown) in the same spectral range for both the DoD RSI and SP paste pads showed that no light was transmitted through the pads printed on a flat glass surface. The spectrum of the DoD RSI pad shows 85–90% reflectance above the characteristic absorption edge of Ag around 310–325 nm, which is lower than the mirror Ag (95–98%); it also shows a distinct dip around 350 nm. These are characteristics of a rough Ag surface [19]. The dip in reflectance is attributed to absorption of the light by surface plasmons on the surface features of the DoD RSI pad, which is negligible for the smooth Ag mirror [19], [20]. Decreased reflectance from 350 to 1200 nm can have a different origin. It can result from scattering of light in the porous metal structure and enhanced absorption or the presence of organic residues, which absorb light. For the entire spectral range shown in Fig. 2, the SP paste pad exhibits lower reflectance than the Ag mirror and the DoD RSI contact pad, which is likely due to presence of absorbing organics and polymers and a lower fraction of Ag particles. Interestingly, the highly reflective nature of the DoD RSI pad could be beneficial for use as back metallization for a Si solar cell, where it also acts as a light reflector to increase absorption in the Si.

Next, SHJ cells were prepared with front-grid electrodes formed from DoD RSI, and from SP paste, as shown in Fig. 3.

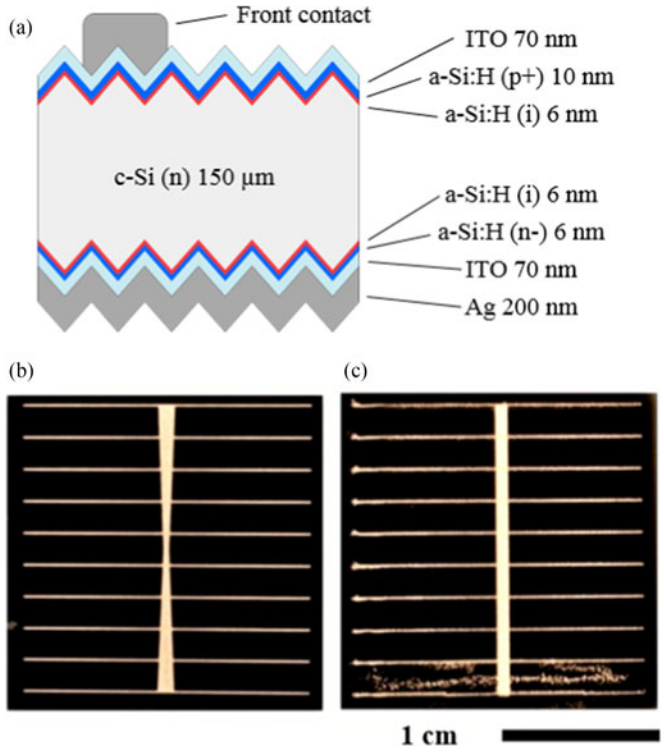

Fig. 3. Schematic of SHJ solar cell layers in cross-sectional (a) contrast-enhanced photograph of SHJ solar cells with front-grid metallization formed from (b) SP paste and (c) DoD RSI.

We emphasize that all solar cells were prepared identically except for the front grid. Fingers for both cells were spaced 2 mm apart; the finger widths and height were 100–130 and 20–25 μm for the SP paste cell, and with larger variability 75–145 and 1–5 μm for the DoD RSI cells, respectively. Note that the fingers width is relatively similar for both types of preparation; however, the SP paste fingers are five to ten times taller. In terms of shadowing, the DoD RSI fingers are on average narrower than SP paste fingers, which should result in lower current generation losses. However, the SP paste cell has a tapered busbar, with an area of $\sim$14 mm^2, compared with 12 mm^2 for DoD RSI cell, respectively. This could overall compensate for finger-width shading effects in current, however slightly higher shading, and thus, lower current generation is expected in the DoD RSI cell. We consider the effect of finger width on solar cell performance as negligible; the difference in width from both types of front-grid metallization is negligible compared with the order of magnitude difference in the media resistivity. Fig. 3(c) also shows additional metallization spots on the bottom region of the DoD RSI cell, originating from instability of the ink droplet formation during printing. These spots act as additional shading, which, if significant, can result in further reduction of photocurrent but should be avoidable with optimization of the printing process.

Fig. 4 shows an SEM cross-sectional image of a DoD RSI finger on an SHJ solar cell. The DoD RSI finger presents a porous morphology of small interconnected spherical particles about 25–250 nm in diameter; this results in nonuniform coverage of the cell surface, leaving areas of the textured pyramid tips exposed. Printing on the textured surface alters the RSI structure as compared with printing on a flat substrate, as the dispensed ink droplets flow to the trough of the textured valleys, between textured pyramids before nucleating. The resulting morphology on textured surface is expected to influence the RSI finger properties. First, in thinner and more porous fingers, current transport via percolation will be limited by the lower order of connectivity of conductive Ag particles, leading to higher resistance [17]. Second, the poor surface coverage between the Ag particles and the ITO surface can alter interfacial specific contact resistance. These two effects can impact the solar cell series resistance. Third, the adhesion and reliability of the metallization might suffer from nonuniform coverage. Finally, the openings through the DoD RSI finger contacts might transmit some light through the peaks to the Si and, hence, allow a beneficial increase in current photogeneration.

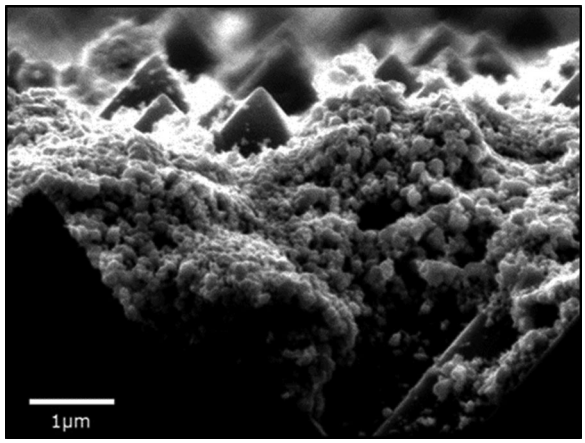

Fig. 4. SEM cross-sectional image of a porous DoD RSI finger on a textured SHJ solar cell.

Ideal solar cell front grids would have minimal electrical resistivity and be completely transparent. In a realistic solar cell, optimization of the front-grid geometries can mitigate the tradeoff between power losses from shading of wide fingers while minimizing the current carrying capacity of fingers with a small cross-sectional area. Solar cell front-grid geometries with narrow fingers of high cross-sectional area (high aspect ratio) are expected to yield the best performance. Interestingly, as discussed below, the solar cells prepared with DoD RSI front grid perform comparably to the SP paste solar cell—with very little process optimization—despite finger geometry with low aspect ratio, high porosity, and poor adhesion, showing that there is room for improvement.

Furthermore, the electrical properties are assessed by evaluating the specific contact resistances (ρ_c) measured by TLMs, and resistance per unit length on fingers formed from DoD RSI and SP paste. The ρ_c values of SP paste to ITO/Si range from 4×10^{-3} to 10×10^{-3} Ω·cm^2, whereas the range of values for DoD RSI fingers to ITO/Si is $1 - 60 \times 10^4$ $\Omega \cdot$ cm^2. These ρ_c values are typical of those reported for Ag pastes [21]. On average, the DoD RSI ρ_c values are one order of magnitude lower, suggesting lower interfacial resistance, which likely linked to

TABLE I
COMPARISON OF SOLAR CELL ELECTRICAL CHARACTERISTICS

	V_{oc} (mV)	J_{sc} (mA/cm^2)	*pFF* (%)	FF (%)	R_s (Ω·cm^2)	η (%)
SP Paste Cell	713	35.9	81.3	76.3	1.1	19.5
DoD-RSI Cell	712	35.5	80.9	72.9	1.8	18.4

the lower media resistivity of the DoD RSI metallization compared with SP paste. Regarding the larger dispersion, we suggest that where the interfacial contact between the DoD RSI Ag particles and ITO is higher, the ρ_c is at the lower end of the range reported, whereas fingers with less interfacial connectivity result in ρ_c in the higher end of the range. We emphasize that the RSI metallizations were formed without the use of adhesion modifiers. Porosity and adhesion of RSI features to ITO are, therefore, the focus of future work to improve specific contact resistance, along with reliability.

Next, resistance of 1-cm-long SP paste and DoD RSI fingers were measured: the SP paste finger resistance was 3.7 Ω, whereas the DoD RSI was 10.2 Ω. Although the bulk media resistivity (see Fig. 1) of the SP paste films—measured on larger pads—is five times higher than the DoD RSI films, the DoD RSI fingers have very low heights of about 1–5 μm and have, therefore, a lower cross-sectional area compared with the SP paste fingers 20–25 μm in height. As mentioned previously, the RSI metallization is expected to be more porous when deposited on a textured surface. Similarly, higher porosity is expected for narrow fingers compared with larger (7×7 mm^2) pads. During printing, ink droplets are staggered, allowing partial overlap of adjacent droplets. Droplet overlap allows filling in of open pores in the metallization. For narrow fingers that are formed with only two staggered droplet lines that overlap, there is less ink droplet overlap than in larger area pads that consist of hundreds of staggered lines, even when printing parameters (i.e., pitch, number of passes of the print head) are the same. The low cross-sectional area and the relatively high porosity result in RSI fingers with higher resistance than SP paste fingers.

Solar cell performance was then evaluated from suns–V_{OC} and one-sun *I–V* electrical responses. In order to compare the effect of front-grid metallization method on solar cell performance, we extract and compare pseudo-fill factors (*pFF*), fill factors (FF), open-circuit voltage (V_{OC}), short-circuit current density (J_{SC}), and series resistance (R_s) (see Table I). Fig. 5 shows the *I–V* characteristics of the SP paste and DoD RSI cells. Suns–V_{OC} *I–V*, used to extract *pFF* and R_s, is a measure of solar cell electrical response without the effects of series resistance [22]. First, both cells exhibit similar *pFF*, the DoD RSI cell *pFF* is 0.4% lower than for the SP paste cell. Therefore, in the absence of R_s, the cells perform comparably, with the DoD RSI cell only at a marginal disadvantage. This difference in *pFF* might originate from minor deviations in reproducibility from sample to sample. Moreover, the SP paste cell and DoD RSI cell demonstrate similar V_{OC} of 713 and 712 mV, and close values of J_{sc} of 35.9 and 35.5 mA/cm^2, for the SP paste versus DoD RSI cell, respectively. Approximately 0.2 mA/cm^2 difference in J_{SC} is expected from the difference in busbar shading

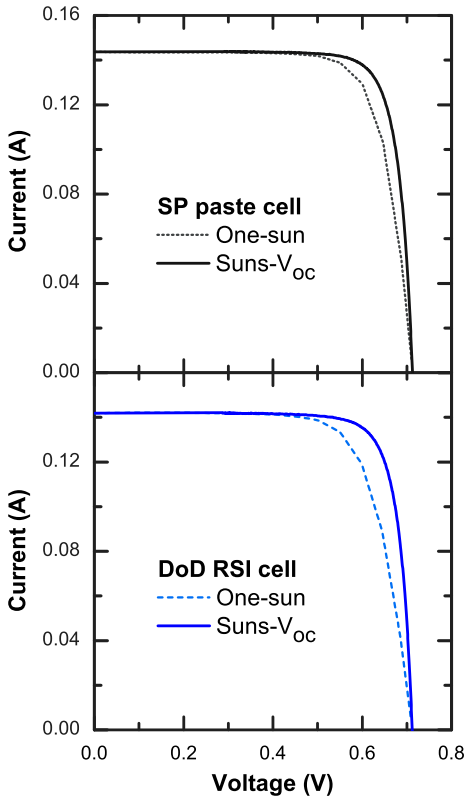

Fig. 5. One-sun and suns–V_{oc} – *I–V* curves for SHJ solar cells with front-grid metallizations formed from SP paste (top) and DoD RSI (bottom).

from the two cells and difference in light reflection off the grid. The remainder of the J_{sc} difference probably originates from additional shading from the extra metallization spots from RSI printing instability [shown in Fig. 3(c)]; it also is possible that this part of the shading was offset by additional absorption of light through the textured peaks that poke through the DoD RSI fingers, as shown in Fig. 4.

The similarity in *pFF*, J_{SC}, and V_{OC} for both types of cells are consistent with the assumption that only the difference in front-grid metallization methods affect R_s. Next, we compare the suns–V_{OC} and one-sun *I–V* responses. This method is one of the most reliable ways to quantify R_s in a solar cell [22], [23]. R_s (see Table I) is calculated from the voltage difference (ΔV) at maximum power point (MPP) from the suns–V_{OC} and one-sun *I–V* curves [23], [24]:

$$R_S = \frac{\Delta V}{J_{\mathrm{MPP,One\,Sun}}}. \tag{1}$$

Solar cell series resistance R_s is a lumped term that is comprised of the resistance of each layer and the interfacial contact

resistance between each layer [25], [26]. Again, since the solar cells in our sample set are prepared identically except for the front-grid metallization method, the difference in R_s can be assumed to only result from differences in resistance of the front grid, and the interfacial contact resistance ρ_c of the front grid to the ITO/Si. Although the lowest ρ_c was demonstrated by the DoD RSI fingers, series resistance losses have only a square root dependence on ρ_c, whereas the series resistance losses scale proportionally with metallization resistance per unit length [25], [26]. Therefore, in our case where ρ_c values have a wide range due to variations in interfacial connectivity of the porous DoD RSI fingers to the ITO, the difference in the resistance of the fingers per unit length $(R_{\rm grid}/L)$ outweighs the benefit of lower average ρ_c. We suggest that this accounts entirely for the slightly lower performance of the cell with the RSI printed finger. This also shows that this is not an intrinsic problem to the DoD RSI metallization but, rather, is linked to the optimization of printing parameters to deposit appropriate thickness and morphology grid on a textured Si and ITO surface.

Finally, we discuss a path toward DoD RSI optimization and exceeding the performance of SP paste. We propose the following path toward improved performance.

1) Approach closer to pure Ag resistivity by reducing porosity, while removing all residual organics by optimizing ink dilution printing parameters and substrate heating.
2) Minimize Ag oxidation by printing in an inert atmosphere.
3) Reduce shadowing from unwanted Ag spots by optimizing the RSI printing parameters for continuous stable droplet formation.
4) Finally, find the optimal power loss tradeoff between porosity, use of adhesion modifiers, features' cross sectional geometry, and possible enhanced photogeneration by transmission of light through the exposed textured peaks of the solar cell, which calls for further investigation.

IV. Summary and Conclusion

DoD printing of RSIs is a low-cost, low-waste, low-thermal budget method that enables formation of highly conductive metallization schemes on temperature-sensitive devices, exemplified in this contribution for SHJ solar cell. We showed that DoD RSI is capable of producing almost pure Ag metal in narrow front grids at temperatures as low as 51 °C, with a high reflectivity and minimum media resistivity of approximately 2.0 $\mu\Omega$·cm. When printed at 78 °C, we showed that a 1:1 (ink:ethanol) RSI recipe yields porous high-purity Ag features, with structure and metal electrode properties depending on printing conditions and substrate morphology. SHJ cells with DoD RSI front-grid electrodes exhibited similar *pFF*, $J_{\rm sc}$, and $V_{\rm oc}$ compared with screen-printed silver paste front electrodes. Cells with DoD RSI front-grid electrodes had series resistance of 1.8 Ω·cm^2 compared with 1.1 Ω·cm^2 for cells with SP paste. This shows that without use of adhesion modifiers or advanced optimization, DoD RSI metallization performs similarly to SP paste metallization that has been custom-designed and commercially produced for this application; it, therefore, offers an alternative to industrially relevant metallization methods.

Furthermore, reactive metal inks, which print a chemical reaction, are expandable for other metals such as Cu, Al, and Ni, thus expanding opportunities for low-temperature metallization for other photovoltaics technologies. Other advanced metallization concepts, such as well-defined patterning of seed layers for electroplating, can also benefit from use of DoD printing of reactive metal inks.

Acknowledgment

A. M. Jeffries would like to thank K. Fisher, M. Boccard, and Z. Yu from the Holman Research Group, Arizona State University, for their valuable discussions and help with sample preparation.

References

[1] S. B. Walker and J. A. Lewis, "Reactive silver inks for patterning high-conductivity features at mild temperatures," *J. Amer. Chem. Soc.*, vol. 134, no. 3, pp. 1419–1421, 2012.
[2] J. Perelaer *et al.*, "Printed electronics: The challenges involved in printing devices, interconnects, and contacts based on inorganic materials," *J. Mater. Chem.*, vol. 20, no. 39, pp. 8446–8453, 2010.
[3] M. A. Green *et al.* "Solar cell efficiency tables (ver. 45)," Prog. Photovolt.: Res. Appl. 23.1, pp. 1–9, Jan. 2015.
[4] M. Taguchi, A. Terakawa, E. Maruyama, and M. Tanaka, "Obtaining a higher Voc in HIT cells," *Prog. Photovoltaics, Res. Appl.*, vol. 13, no. 6, pp. 481–488, Sep. 2005.
[5] D. Li, D. Sutton, A. Burgess, D. Graham, and P. D. Calvert, "Conductive copper and nickel lines via reactive inkjet printing," *J. Mater. Chem.*, vol. 19, no. 22, pp. 3719–3724, 2009.
[6] O. Lefky, C. S. Mamidanna, A. Huang, and Y. Hildreth, "Impact of solvent selection and temperature on porosity and resistance of printed self- reducing silver inks," *Phys. Status Solidi Appl. Mater. Sci.*, vol. 213, pp. 2751–2758, 2016.
[7] W. M. Haynes, *CRC Handbook of Chemistry and Physics*, 95th ed. Boca Raton, FL, USA: CRC, 2014.
[8] H. Meier, U. Löffelmann, D. Mager, P. J. Smith, and J. G. Korvink, "Inkjet-printed, conductive, 25 μm wide silver tracks on unstructured polyimide," *Phys. Status Solidi Appl. Mater. Sci.*, vol. 206, no. 7, pp. 1626–1630, 2009.
[9] S. De Wolf, A. Descoeudres, Z. C. Holman, and C. Ballif, "High-efficiency silicon heterojunction solar cells: A review," *Green*, vol. 2, pp. 7–24, 2012.
[10] P. Chien *et al.*, "Metallization optimization for high efficiency silicon heterojunction solar cells using low-temperature paste screen printing," in *Proc. 39th IEEE Photovoltaics Spec. Conf.*, 2013, pp. 2187–2190.
[11] S. De Wolf and M. Kondo, "Nature of doped a-Si:H/c-Si interface recombination," *J. Appl. Phys.*, vol. 105, 2009, Art. no. 103707.
[12] Y. Tao, Y. Tao, B. Wang, L. Wang, and Y. Tai, "A facile approach to a silver conductive ink with high performance for macroelectronics," *Nanoscale Res. Lett.*, vol. 8, no. 1, pp. 1–6, 2013.
[13] Y. Hermans *et al.*, "Advanced metallization concepts by inkjet printing," in *Proc. 29th Eur. Photovoltaic Sol. Energy Conf. Exhib.*, 2000, pp. 518–522.
[14] L. Hock, "Inkjet printing gone solar," *R & D Mag.*, Aug. 2015. [Online]. Available: https://www.rdmag.com, Accessed on: May 2016.
[15] T. Shanmugam *et al.*, "Analysis of fine-line screen and stencil-printed metal contacts for silicon wafer solar cells," *IEEE J. Photovoltaics*, vol. 5, no. 2, pp. 525–533, Mar. 2015.
[16] B. Demaurex, S. De Wolf, A. Descoeudres, Z. C. Holman, and C. Ballif, "Damage at hydrogenated amorphous/crystalline silicon interfaces by indium tin oxide overlayer sputtering," *Appl. Phys. Lett.*, vol. 101, no. 17, 2012, Art. no. 171604.
[17] D. S. McLachlan, M. Blaszkiewicz, and R. E. Newnham, "Electrical resistivity of composites," *J. Amer. Ceram. Soc.*, vol. 73, no. 8, pp. 2187–2203, Aug. 1990.
[18] V. Shapovalov, "Porous metals," *MRS Bull.*, vol. 19, no. 4, pp. 24–28, Apr. 1994.
[19] L. J. Cunningham and A. J. Braundmeier, "Measurement of the correlation between the specular reflectance and surface roughness of Ag films," *Phys. Rev. B*, vol. 14, no. 2, pp. 479–483, Jul. 1976.

[20] G. Rasigni, F. Varnier, M. Rasigni, J. P. Palmari, and A. Llebaria, "Roughness spectrum and surface plasmons for surfaces of silver, copper, gold, and magnesium deposits," *Phys. Rev. B*, vol. 27, no. 2, pp. 819–830, Jan. 1983.
[21] M. Marinkovic, "Contact resistance effects in thin film solar cells and thin film transistors," Ph.D. dissertation, Dept. Elect. Eng., Jacobs Univ. Bremen, Bremen, Germany, 2013.
[22] R. Sinton and A. Cuevas, "A quasi-steady-state open-circuit voltage method for solar cell characterization," in *Proc. 16th Eur. Photovoltaics Sol. Energy Conf.*, May 2000, pp. 1–4.
[23] D. Pysch, A. Mette, and S. W. Glunz, "A review and comparison of different methods to determine the series resistance of solar cells," *Sol. Energy Mater. Sol. Cells,* vol. 91, no. 18, pp. 1698–1706, 2007.
[24] M. Wolf and H. Rauschenbach, "Series resistance effects on solar cell measurements," *Adv. Energy Convers.*, vol. 3, no. 2, pp. 455–479, 1963.
[25] S. R. Aberle, A. G. Wenham, and M. A. Green, "Series resistance of solar cells," in *Proc. IEEE Photovoltaic Spec. Conf.*, 1993, pp. 133–139.
[26] D. L. Meier and D. K. Schroder, "Contact resistance: Its measurement and relative importance to power loss in a solar cell," *IEEE Trans. Electron Devices*, vol. ED-31, no. 5, pp. 647–653, May 1984.

Authors' photographs and biographies not available at the time of publication.